Viscosity of Interfacial Water

Yingxi Zhu and Steve Granick

Department of Materials Science and Engineering, University of Illinois, Urbana, Illinois 61801

(Received 6 February 2001; published 10 August 2001)

The effective shear viscosity and frequency-dependent dynamic oscillatory shear spectra of water containing monovalent or divalent ions (ionic strength 25 mM), confined between mica crystals at 1–2 water molecules thickness, oscillated with twist angle with the period expected for the pseudohexagonal surface lattice. The effective viscosity varied by orders of magnitude as the twist angle was changed. Confinement appeared to imprint lateral spatial correlation on the ultrathin liquid, the more so the better the confining lattices were aligned, but the oft-proposed "ice structure" was not observed dynamically.

DOI: 10.1103/PhysRevLett.87.096104 PACS numbers: 68.08.–p, 68.35.Md

The role of water in physical situations from geology to biology is almost universally thought to be important but the details are disputed. We are especially interested in water that adjoins charged solids when they are brought close together. In a distal regime, thickness is large enough that continuum-based theories can be expected to apply, as embodied in the DLVO (Derjaguin-Landau-Verwey-Overbeek) theory [1]. There is also a proximal regime, within a few molecular dimensions of a solid surface, where the confined aqueous fluid is no longer usefully regarded as a continuum and its molecular granularity can be expected to come into play [2]. This is the "Stern" layer of colloid science. What is the structure of interfacial water? What of the associated transport properties: What is the viscosity of water within the Stern layer?

Pursuit of this controversial question led in the past to the infamous "polywater" saga in which water anomalies in quartz or pyrex capillaries were eventually traced to contaminants [3]—and we are mindful of this. At the same time there is evidence that water in clay-water systems has an elevated viscosity [4] and that this is independent of the specific nature of the surface, resulting essentially from geometrical confinement [5]. Our initial experiments to test these ideas were based on analyzing the hydrodynamic forces that resist drainage when the surface spacing changes dynamically. It emerged that the traditional Reynolds lubrication equation, in which hydrodynamic forces diverge with film thickness [6], fails when the flow rate is rapid (presumably owing to flow-induced separation of dissolved ions), as will be described elsewhere. To simplify the situation, here we consider shear deformations in the regime of linear response. Linear responses ensured that the experiment would not in itself order or disorder the films. As described below, differences between our initial irreproducible experiments were traced to differences between the angle between the crystalline confining surfaces, whose mutual orientation we shall refer to as "twist angle."

The atomically smooth clay surfaces (muscovite mica) used in this study are pseudohexagonal (a monoclinic crystal structure cleaved along its 001 plane). Immersed in water, they become negatively charged when cleavage exposes interstitial K^+ ions that first become randomly distributed between the cleaved surfaces, and then dissolve in water [7]. The mica sheets were brought to the spacing of 1–2 monolayers (see below). In this confined geometry, we expect the local counterion concentration to have been of order twice the surface charge to keep the total charge approximately neutral. The local charge concentration was then of order 15 M—tremendously larger than would be characteristic of ions in bulk aqueous solution. In this study, we held the solution's ionic strength at 25 mM but the same would apply even if the water were nominally deionized. The large local concentration of ions results from the need for electroneutrality and is a characteristic feature of aqueous fluids confined between charged surfaces in close proximity.

The starting point was to measure anisotropy of friction when sliding was parallel to the optic axis of one of the surfaces. By discriminating the in-phase (elastic) and the out-of-phase (viscous) responses to harmonic shear, the frequency dependence of the viscoelastic spectra was quantified. For this purpose, the modification of a surface force apparatus was described previously [8–10]. A droplet of aqueous electrolyte was placed between two crossed cylindrical lenses. With compression, the cylinders became flattened at their point of contact, simplifying the local geometry to flat parallel plates. Multiple beam interferometry was used to measure the separation. Piezoelectric bimorphs were used to produce and detect controlled shear motions. The water was passed through a purification system (Barnstead) and then mixed to the desired molarity with analar (>99.9%) grade salts (Aldrich). The temperature was 25 °C.

For comparison with the literature, the static force-distance profiles were also measured, as illustrated in Fig. 1. Figure 1 shows data for monovalent and divalent salts, $NaNO_3$ and $CaCl_2$. Forces $F(D)$ at spacing D are normalized by R, the radius of curvature (≈2 cm). These data agree with the literature [1,11]. The repulsive forces in the distal regime follow the expected decay length, the Debye length at this ionic strength (see the figure caption). The new point was to explore shear forces in the proximal regime. Included in Fig. 1 are the shear forces of $CaCl_2$ solutions measured at one frequency.

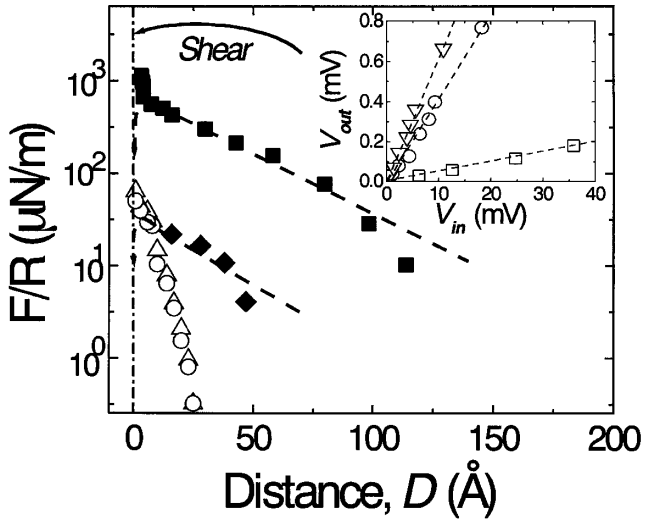

FIG. 1. Static forces (filled symbols) and shear forces (open symbols), both normalized by radius of curvature, R, are plotted against film thickness for an aqueous droplet of $NaNO_3$ (25 mM; squares) and $CaCl_2$ (10 mM; diamonds) at mica twist angle $\theta = 5 \pm 2°$. The dashed lines show the expected DLVO decay lengths of 19 and 17 Å, respectively. The static forces were monotonically repulsive for $NaNO_3$ but, for $CaCl_2$, van der Waals attraction caused the surfaces to jump from $D \approx 2$ nm into an attractive minimum at $D = 2 \pm 2$ Å from which the jump-out force gave adhesion $F/R \approx 36\ \mathrm{mN\,m^{-1}}$. The shear forces, viscous (triangles) and elastic (circles), concern the $CaCl_2$ situation at 1.3 Hz and amplitude 2 Å (note that the shear forces were measured dynamically during the jump into contact). The inset demonstrates linearity for 10 mM $CaCl_2$ at thickness 2 ± 2 Å. In the piezoelectric force-sensing device, the sensor voltage (V_{out}) is plotted against input voltage (V_{in}) at 1.3, 10, and 40 Hz, respectively, for squares, circles, and triangles. Shear measurements reported in the following figures were performed at $V_{\mathrm{in}} = 10$ mV, safely within the regime of linear response.

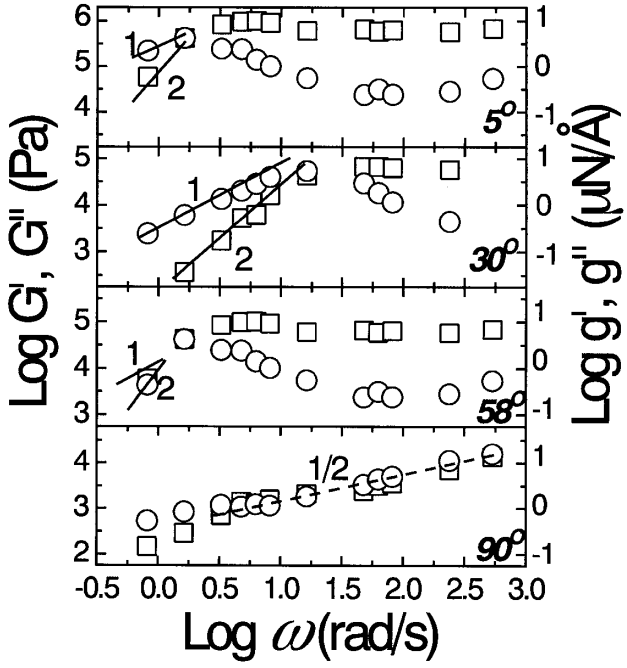

FIG. 2. For the twist angles $\theta = (5 \pm 2)°$, $(30 \pm 2)°$, $(58 \pm 2)°$, and $(90 \pm 2)°$ shown, the linear viscoelastic shear spectrum is plotted on log-log scales against angular frequency for 25 mM aqueous $CaCl_2$ at $D = 2 \pm 2$ Å. On the left-hand ordinate are plotted the effective loss modulus, G'' (circles) and effective elastic modulus, G' (squares). On the right-hand ordinate scale are the viscous, g'' (circles), and elastic, g' (squares), forces with units of μN per angstrom deflection. Lines with slopes 1 and 2 are drawn as guides to the eye.

The shear responses were immeasurably small except at $D < 20$–25 Å, confirming the traditional view that water structure in the distal region is essentially the same as in the bulk. The inset illustrates that this was linear response.

We then focused on frequency dependence. The experiments were stable—neither the shear spectrum nor the thickness changed when the normal pressure was varied over a wide range, 3–5 MPa. Considering that the characteristic dimension of the water molecule in a molecularly thin film is ≈2.5 Å [12], and taking into account the unavoidable uncertainty in determining the film thickness, the measured thickness of $D = 2 \pm 2$ Å amounted to 1–2 water molecules, i.e., 1–2 monolayers. In Fig. 2, four examples are shown in which the film thickness was the same but the twist angle was varied (5°, 30°, 58°, and 90°). In Fig. 2, shear forces have been normalized in two alternative ways. The right-hand ordinate scale shows viscous and elastic forces with units of force per angstrom of shear motion. Additional normalization for film thickness and contact area gave the effective loss modulus, $G''(\omega)$, and elastic modulus, $G'(\omega)$ (left ordinate), where ω denotes radian frequency.

These viscoelastic shear spectra evidently differ considerably, in magnitude and shape, according to the twist angle. It is well-known from rheology that a system whose dynamical structure is characterized by a dominant relaxation time has constant G' when the drive frequency exceeds this inverse time and that, at lesser frequencies, $G'' \sim \omega$ and $G' \sim \omega^2$ according to the Kramers-Kronig relations [13]. While it is true that the expected low-frequency power-law frequency response was not always seen clearly over the accessible frequency window, a peak in $G''(\omega)$ at low frequency was always observed except at 90° twist angle (see below), demonstrating the presence of a prominent low-frequency relaxation process. For further analysis, this was quantified as the frequency, ω_0, where elastic and viscous responses crossed. This defined the fluid's terminal relaxation time, $\tau_0 \equiv 2\pi/\omega_0$. Therefore, unlike nonpolar fluids confined to comparable spacings of 1–2 molecules [8,14,15], these confined aqueous films failed to "solidify." [The mechanical signature of solidification is that G' is finite at zero frequency. Operationally, it would be that $G''(\omega)/G'(\omega) \ll 1$ at every accessible ω, which was not observed either.]

Therefore the shear responses were fluid but with response times much retarded relative to those of bulk water, whose response is in picoseconds. This is consistent with our earlier experiments in which the twist angle was not controlled [9], with recent AFM (atomic force microscope) friction experiments [16], and is broadly consistent with the fact that aqueous solutions display low kinetic friction [17]. Previously, we attributed the confinement-induced slowing-down of nonpolar fluids to the glassy packing and crowding of molecules within a restricted space [14]. This picture of caged motion is also broadly consistent with the present findings but requires additional interpretation as concerns twist angle (see below).

At most of the twist angles, the shear spectra could be described by one dominant relaxation over the accessible frequency range: a peak in $G''(\omega)$ followed by a region where $G'(\omega)$ was constant. The exception was the twist angle of 90°, where the moduli were exceptionally small and $G'(\omega) \approx G''(\omega) \sim \omega^{1/2}$. By known arguments [13], this indicated a wide distribution of relaxation times rather than any single dominant one. It is tantalizing that $\omega^{1/2}$ scaling is phenomenologically like the "Rouse" behavior [13] that describes the normal modes of a linear series of beads and springs. This suggests, by arguments described below, some kind of strong coupling between different structural subunits within the Moiré pattern produced by two pseudohexagonal surface lattices at right angles to one another, but no quantitative interpretation is offered at this time.

It is known from linear rheology that a fluid's low-frequency viscosity is $\eta \equiv G''(\omega)/\omega$ in the regime $G'' \sim \omega$. Figure 3 (top panel) summarizes a large family of shear measurements in which the twist angle was varied from ~0° to ~90°. On the left-hand ordinate axis, the terminal relaxation time, τ_0 is plotted the effective viscosity, $\eta_{\text{eff}} \equiv G''(\omega_0)/\omega_0$. It is evident that both η_{eff} and τ_0 oscillated by orders of magnitude with the period of 60° expected for a hexagonal lattice. However, the results obtained at multiples of 60° were slightly different — more so than could be explained by uncertainty in determining twist angle. This is probably related to the pseudohexagonal character of mica noted above. In addition, data for τ_0 at 30° and 90° scattered by a factor of 100, between 10^{-1} and 10^{-3} s, within our experimental uncertainty of ±2° twist angle. The same holds for adhesion: Sensitivity to small (±1°) changes in twist angle is known concerning the adhesion of molecularly thin H_2O and aqueous KCl solutions [7].

We now turn speculatively to structural interpretation. If these effects had involved the localization of counterions to the charged mica lattice, whose unit of charge is monovalent, divalent counterions should be produced effects different from monovalent ones. Figure 3 shows no difference between Ca^{2+} and Na^+, however. Mismatch between the unit of charge on the lattice and the counterions appeared not to matter. (But, parenthetically, K^+ salts systematically show lower η_{eff} and shorter τ_0, by 1–2 orders of magnitude. The difference from Na^+ is not understood at this time.)

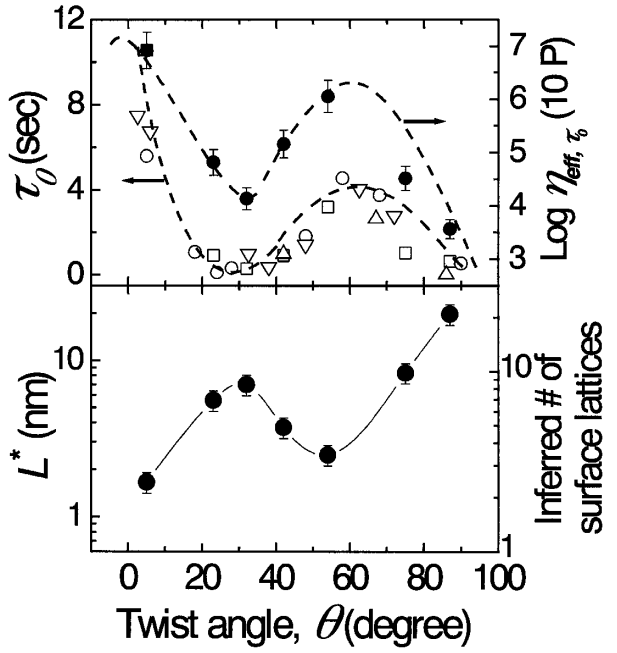

FIG. 3. (Top panel) Terminal relaxation time, τ_0 (left ordinate), and effective viscosity η_{eff} (right ordinate) plotted against twist angle for aqueous films 2 ± 2 Å thick. Three aqueous solutions were studied, all at the same ionic strength, 25 mM, but containing either monovalent or divalent cations: $NaNO_3$ (squares), $MgCl_2$ (triangles), and $CaCl_2$ (circles). To render relative data most comparable, the $CaCl_2$ solutions were measured in the same experiment. The error bars are based on the statistics of additional data obtained using other electrolyte solutions, including other ions not shown here. Dashed lines indicate the expected period for a hexagonal lattice. (Bottom panel) Inferred domain size, L^* (left ordinate), and equivalent number of mica unit cells (right ordinate), inferred from the shear modulus as described in the text, are plotted for $CaCl_2$ solutions measured in the same experiment in order to render the data most comparable quantitatively. There is overall uncertainty in the ordinate scale by a factor of 2–5, owing mainly to uncertainty in determining the film thickness, but this did not affect relative error because the experiment was the same. The indicated error bars refer to relative error.

The *magnitudes* of moduli in Fig. 3 are "soft." The following tentative argument was used to estimate the cooperativity volume responsible. The energy intensity of Brownian motion is k_BT (k_B is the Boltzmann constant and T is the absolute temperature). The shear modulus (dimension force-area^{-1}) is dimensionally energy-volume^{-1}. Division by the film thickness gave energy-area^{-1}, or, equivalently, the surface area attributable to $1k_BT$ of stored energy at the crossover frequency of terminal relaxation where η_{eff} was evaluated. The calculation is admittedly qualitative, but it is worth emphasizing that a similar approach is standard for colloidal systems, where the shear modulus of a hard sphere colloid is inversely proportional to its diameter cubed [18], and in fluid polymer systems,

where the entanglement modulus is inversely proportional to the mesh size cubed [13]. There is, in principle, also a higher-frequency shear modulus (at frequencies too high to be visible over our frequency window), in addition to the soft low-frequency process probed in these experiments.

On physical grounds, we interpret this calculation to estimate the distance that confined molecules can move relatively freely before becoming obstructed by the solid's surface potential. The implied lateral length scale, L^*, which is the square root of the area calculated from the argument in the previous paragraph, is plotted in Fig. 3 (bottom panel) as a function of twist angle (left-hand ordinate). The equivalent number of surface lattice dimensions is also shown (right-hand ordinate). Twist angle dependence could not be observed, however, for films three monolayers thick or more ($D \geq 6$ Å)—at those larger dimensions, the intrinsic liquid structure apparently dominated.

The epitaxial organization of fluids next to solid surfaces has long been predicted from computer simulations of Lennard-Jones particles and molecules [19–22] and these findings appear to confirm these predictions qualitatively. A significant difference is that, unlike the available simulations [19–22], the surface lattice dimension was much larger than the size of the fluid molecules.

These aqueous systems present decidedly more complex intermolecular forces and local electric fields than the confined nonpolar systems that have been much studied. The orientation of water at the solid-liquid interface, and the expected surface-induced changes in hydrogen-bonding structure [23] have no counterpart for nonpolar fluids. We emphasize that, although the solid surfaces appeared to imprint spatial correlations (order) on the interfacial water, resulting in a large effective viscosity, the oft-proposed "ice structure" [24] was not observed dynamically. These issues are relevant to colloidal suspensions, soil science, and geophysics, and have possible ramifications for understanding vicinal water at lipids and proteins.

We thank Kenneth S. Schweizer and Peter Harrowell for comments. This work was supported in part by National Science Foundation (Tribology Program) with the use of facilities provided by the U.S. Department of Energy, Division of Materials Science, under Award No. DEFG9645439 to the Frederick Seitz Materials Research Laboratory at the University of Illinois at Urbana-Champaign.

[1] J. N. Israelachvili, *Intermolecular and Surface Forces* (Academic, London, 1991), 2nd ed.
[2] J. N. Israelachvili and H. Wennerstrom, Nature (London) **379**, 219 (1996).
[3] B. V. Derjaguin, Z. M. Zorin, Ya. I. Rabinovich, and N. V. Churaev, J. Colloid Interface Sci. **46**, 437 (1974).
[4] P. F. Low, Soil Sci. Soc. Am. J. **40**, 500 (1976).
[5] Y. Sun, H. Lin, and P. F. Low, J. Colloid Interface Sci. **112**, 556 (1986).
[6] J. N. Israelachvili, J. Colloid Interface Sci. **110**, 263 (1986).
[7] P. M. McGuiggan and J. N. Israelachvili, J. Mater. Res. **5**, 2232 (1990).
[8] J. Van Alsten and S. Granick, Phys. Rev. Lett. **61**, 2570 (1988).
[9] A. Dhinojwala and S. Granick, J. Am. Chem. Soc. **119**, 241 (1997).
[10] M. Ruths and S. Granick, Langmuir **16**, 8368 (2000).
[11] P. M. Claesson, P. Herder, P. Stenius, J. C. Eriksson, and R. M. Pashley, J. Colloid Interface Sci. **109**, 31 (1986); R. M. Pashley, J. Colloid Interface Sci. **83**, 531 (1981); R. M. Pashley and J. N. Israelachvili, J. Colloid Interface Sci. **97**, 446 (1984).
[12] J. N. Israelachvili and R. M. Pashley, Nature (London) **306**, 249 (1983).
[13] J. D. Ferry, *Viscoelastic Properties of Polymers* (Wiley, New York, 1982), 3rd ed.
[14] A. L. Demirel and S. Granick, Phys. Rev. Lett. **77**, 2261 (1996).
[15] B. Bhushan, J. N. Israelachvili, and U. Landman, Nature (London) **374**, 607 (1995).
[16] M. Antognozzi, A. D. L. Humphris, and M. J. Miles, Appl. Phys. Lett. **78**, 300 (2001).
[17] A. M. Homola, J. N. Israelachvili, M. L. Gee, and P. M. McGuiggan, ASME J. Tribol. **111**, 675 (1989).
[18] W. B. Russel, D. A. Saville, and W. B. Schowalter, *Colloidal Dispersions* (Cambridge University Press, New York, 1989).
[19] M. Schoen, Jr., C. L. Rhykerd, D. J. Diestler, and J. H. Cushman, Science **245**, 1223 (1989).
[20] M. Cieplak, E. D. Smith, and M. O. Robbins, Science **265**, 1209 (1994).
[21] J. P. Gao, W. D. Luedtke, and U. Landman, Phys. Rev. Lett. **79**, 705 (1997).
[22] G. He, M. Müser, and M. O. Robbins, Science **284**, 1650 (1999).
[23] H. Bluhm, T. Inoue, and M. Salmeron, Phys. Rev. B **61**, 7760 (2000); M. F. Toney *et al.,* Nature (London) **368**, 444 (1994); X. C. Su, L. Lianos, Y. R. Shen, and G. A. Somorjai, Phys. Rev. Lett. **80**, 1533 (1998); K. Koga, H. Tanaka, and X. C. Zeng, Nature (London) **408**, 564 (2000); C. Y. Lee, J. A. McCammon, and P. J. Rossky, J. Chem. Phys. **80**, 4448 (1984).
[24] P. M. Wiggins, Microbiol. Rev. **54**, 432 (1990); M. Odelius, M. Bernasconi, and M. Parrinello, Phys. Rev. Lett. **78**, 2855 (1977); W. Cantrell and G. E. Ewing, J. Phys. Chem. B **105**, 5434 (2001).